Gene Expression-Based Molecular Diagnostic System for Malignant Gliomas Is Superior to Histological Diagnosis

Mitsuaki Shirahata,[1,2] Kyoko Iwao-Koizumi,[2] Sakae Saito,[2] Noriko Ueno,[2] Masashi Oda,[1] Nobuo Hashimoto,[1] Jun A. Takahashi,[1] and Kikuya Kato[2]

Abstract

Purpose: Current morphology-based glioma classification methods do not adequately reflect the complex biology of gliomas, thus limiting their prognostic ability. In this study, we focused on anaplastic oligodendroglioma and glioblastoma, which typically follow distinct clinical courses. Our goal was to construct a clinically useful molecular diagnostic system based on gene expression profiling.

Experimental Design: The expression of 3,456 genes in 32 patients, 12 and 20 of whom had prognostically distinct anaplastic oligodendroglioma and glioblastoma, respectively, was measured by PCR array. Next to unsupervised methods, we did supervised analysis using a weighted voting algorithm to construct a diagnostic system discriminating anaplastic oligodendroglioma from glioblastoma. The diagnostic accuracy of this system was evaluated by leave-one-out cross-validation. The clinical utility was tested on a microarray-based data set of 50 malignant gliomas from a previous study.

Results: Unsupervised analysis showed divergent global gene expression patterns between the two tumor classes. A supervised binary classification model showed 100% (95% confidence interval, 89.4-100%) diagnostic accuracy by leave-one-out cross-validation using 168 diagnostic genes. Applied to a gene expression data set from a previous study, our model correlated better with outcome than histologic diagnosis, and also displayed 96.6% (28 of 29) consistency with the molecular classification scheme used for these histologically controversial gliomas in the original article. Furthermore, we observed that histologically diagnosed glioblastoma samples that shared anaplastic oligodendroglioma molecular characteristics tended to be associated with longer survival.

Conclusions: Our molecular diagnostic system showed reproducible clinical utility and prognostic ability superior to traditional histopathologic diagnosis for malignant glioma.

Malignant gliomas are the most common primary malignant brain tumors. The current treatment strategy for malignant gliomas consists of maximum surgical resection followed by radiation therapy combined with chemotherapy. Despite these aggressive therapeutic interventions, these tumors are still difficult to eliminate because of their highly malignant character. Their diffusely infiltrative growth pattern limits the extent of safe surgical resection, and they are often resistant to chemotherapeutic adjuvant therapy. However, the severity of these malignant properties differs between the different histologic types of malignant gliomas.

Currently, the most widely used classification scheme for human glioma is that of the WHO (1). For classic glioma cases with typical morphologic features, histologic diagnoses are generally consistent and accurately predict the corresponding clinical course. However, many gliomas do not fit neatly into any of the WHO categories due to their atypical histologic features. Additionally, because the WHO classification schemes are based largely on visual criteria, they are inevitably subject to considerable interobserver variation (2). As a result, the more atypical a glioma, the more likely that the clinical outcome will fail to match the predicted biological behavior. Generally, there is a distinct prognostic difference between patients with glioblastoma and anaplastic oligodendroglioma (1). However, the clinical task is more complex than merely separating malignant gliomas into these two groups with distinct malignant properties, and the findings to date indicate the essential limitations of current glioma classification schemes (3).

Ideally, tumor diagnosis should be objective, and to the extent to which it is possible, it should correctly reflect the biological behavior and corresponding outcome. Recently, genetic analyses showed that allelic loss of chromosomes 1p and 19q was significantly associated with prolonged survival in

Authors' Affiliations: [1]Department of Neurosurgery, Graduate School of Medicine, Kyoto University, Kyoto, Japan and [2]Osaka Medical Center for Cancer and Cardiovascular Diseases, Osaka, Japan

Received 11/27/06; revised 6/22/07; accepted 9/26/07.

Grant support: Grant-in-Aid for the Development of Innovative Technology from the Ministry of Education, Culture, Sports, Science and Technology of Japan.

The costs of publication of this article were defrayed in part by the payment of page charges. This article must therefore be hereby marked *advertisement* in accordance with 18 U.S.C. Section 1734 solely to indicate this fact.

Note: Supplementary data for this article are available at Clinical Cancer Research Online (http://clincancerres.aacrjournals.org/).

Requests for reprints: Kikuya Kato, Osaka Medical Center for Cancer and Cardiovascular Diseases, 1-3-2, Nakamichi, Higashinari-ku, Osaka 537-8511, Japan. E-mail: katou-ki@mc.pref.osaka.jp.

doi:10.1158/1078-0432.CCR-06-2789

anaplastic oligodendroglioma (4). This finding highlights the importance of classifying gliomas into molecularly distinct groups, a prospect that should allow for markedly increased predictive power in the future.

Thus far, we have done gene expression profiling of a total of 1,200 human cancers using adaptor-tagged competitive PCR (ATAC-PCR), a PCR array system based on a high throughput reverse transcription-PCR technique (5–7), and have constructed a cancer gene expression database that is open to the public (8). In this study, we did gene expression profiling on malignant gliomas to construct a prognostically useful diagnostic system for discriminating anaplastic oligodendroglioma from glioblastoma. The clinical utility of this system was then tested on the microarray-based public data set, which includes outcome information.

Materials and Methods

Samples and RNA/DNA isolation. In all cases, tumor specimens were dissected into two portions at surgery, one for histologic diagnosis and the other for molecular research. Histologic diagnosis was done on formalin-fixed, paraffin-embedded tissues. Tumor specimens for molecular research were snap frozen immediately at surgical resection and kept at -80°C until use. Total RNA was extracted from 100 mg of tumor specimens with TRIzol reagent (Invitrogen) according to the manufacturer's instructions. When total RNA was extracted from every tumor specimen, adjacent portions of tumors were sectioned for histologic reconfirmation. Tumor specimens containing 20% or more of nontumor or necrotic area were excluded for further analysis. Genomic DNA was isolated from tumor specimens using QIAamp DNA Mini Kit (Qiagen GmbH) according to the manufacturer's instructions. The study protocol was approved by the institutional review board of Kyoto University, and written informed consent was obtained from each of the patients.

Random expressed sequence tag sequencing, ATAC-PCR assay, and data processing. The expression of 3,456 genes was measured by PCR array via the ATAC-PCR method. The selection of objective genes for measurement was based on an expressed sequence tag sequencing survey of the genes expressed in 12 glioma tissues as previously described (9). We obtained 3,012 unique sequences from the EST collection and prepared 3,456 primers for ATAC-PCR, including additional 444 genes selected from a literature survey. Use of tissue-specific genes avoided wasteful measurement of genes not detected in glioma tissues, providing the advantage of reducing noise in the statistical analysis. The ATAC-PCR experimental procedure was done as previously described (7). The raw value describing gene expression levels were divided by the median expression value of each sample. This standardization step corrects for variation in mRNA level from sample to sample. Values <0.05 and >20 were converted to 0.05 and 20, respectively, and subsequently the entire data matrix was converted to a logarithmic scale. The detailed protocols for the ATAC-PCR experimental procedure are available on our Web site. The complete list of genes and expression data collected and analyzed in this study are available as Supplementary Data. The data will be deposited in Center for Information Biology Gene Expression Database in the DNA Data Bank of Japan.

Methylation-specific PCR, loss of heterozygosity analysis of 1p and 19q, and mutation analysis. DNA methylation patterns in the CpG island of the *MGMT* gene was determined by the method of methylation-specific PCR as previously described (10, 11). Genotypes for multiple loci for loss of heterozygosity analysis were determined by PCR using fluorescent primers tagged with FAM (Hokkaido system science) for microsatellite markers on chromosome 1p36 and 19q13 as previously described (12, 13). *P53* mutation status was analyzed by sequencing between exons 4 and 10, including the DNA-binding domain as previously described (14). *EGFRvIII* was detected by reverse transcription-PCR as previously described (15).

Statistical analysis. Hierarchical cluster analysis and principal component analysis were done using Genmath2.0 software. For the hierarchical cluster analysis, the Ward clustering method was adopted, with Euclid distance used as a similarity coefficient.

The statistical significance of the anaplastic oligodendroglioma/glioblastoma comparison was evaluated for each gene by both P value and q value analysis. The P value of a test measures the minimum false-positive rate that is incurred when calling that test significant. Likewise, the q value of a test measures the minimum false-discovery rate that is incurred when calling that test significant. The false-discovery rate is the expected proportion of false positives among the tests found to be significant (16). The P values were calculated using t statistics. The q values were calculated using the software "Qvalue," supplied online.[3]

To construct a molecular diagnostic system to discriminate anaplastic oligodendroglioma from glioblastoma, we used a weighted voting algorithm coupled with gene selection using signal-to-noise ratio ranking. The weighted voting algorithm is a popular supervised learning method with excellent predictive ability for binary classification using gene expression data (17). Briefly, we calculated the signal-to-noise ratio (S), $S = (U_{gb} - U_{ao}) / (\sigma_{gb} + \sigma_{ao})$, where U and σ represent the mean and SD of expression for each class glioblastoma and anaplastic oligodendroglioma, respectively. The magnitude of the gene vote (V) reflects the deviation of the test sample X value from the average of glioblastoma and anaplastic oligodendroglioma.

$$V = S(X - (U_{gb} + U_{ao})/2)$$

We summed the V values to obtain the total votes for glioblastoma and anaplastic oligodendroglioma. The prediction strength (PS) for each sample was defined as: $PS = (V_{gb} - |V_{ao}|) / (V_{gb} + |V_{ao}|)$. We adopted a threshold of 0. Samples with PS <0 were judged to be anaplastic oligodendroglioma, whereas those with PS >0 were designated glioblastoma. This model was evaluated by leave-one-out cross-validation. Briefly, one sample was randomly withheld, and the withheld sample was diagnosed using the model that was regenerated using the remaining samples. This process was repeated until every sample was tested and the total diagnostic accuracy was recorded. We chose the optimal number of classifier genes as that demonstrating the best performance by leave-one-out cross-validation.

The functional group analysis estimated the chance of association to a functional group using binomial distribution, described as follows.

$$P_{ao} = 1 - \sum_{X=0}^{M-1} (p/3,269)^{\wedge} x \times (1 - p/3,269)^{\wedge}(87 - x)$$

$$P_{gb} = 1 - \sum_{X=0}^{N-1} (p/3,269)^{\wedge} x \times (1 - p/3,269)^{\wedge}(81 - x)$$

where M, N, and p are the number of genes within the functional group among the classifier genes showing higher expression in anaplastic oligodendroglioma cases, that among the classifier genes showing higher expression in glioblastoma cases, and that among the total population, respectively.

The functional group was based on the Biological Process Ontology Guidelines from the Gene Ontology database. The chromosomal position of each gene was based on the RefSeq database.

We obtained the gene expression data of 50 malignant gliomas from a previously published microarray study from the Massachusetts General Hospital (MGH). The processing of the original raw data was done as follows. From the original raw data set, we judged the 9,285 genes that had been "present" in two or more samples to be eligible for further analysis (18). The expression value of each gene was divided by its median expression level among the samples. Values below 0.01 and above 100 were converted to 0.01 and 100, respectively, and

[3] http://faculty.washington.edu/~jstorey/qvalue/

subsequently the entire data matrix was converted to a logarithmic scale. Cumulative overall survival rates were calculated by the Kaplan-Meier method, and the differences in the survival curves were estimated by the log-rank test, using SPSS software.

We applied the classifier genes in the MGH study to our data set. Classification by *K*-nearest neighbor was done with $K = 3$ and Euclidean distance as the similarity measure. The diagnostic accuracy was evaluated by leave-one-out cross-validation.

Results

Sample characteristics. Thirty-two glioma specimens (12 anaplastic oligodendrogliomas and 20 glioblastomas) were obtained from patients who underwent surgical resection at Kyoto University Hospital or nearby regional hospitals between 1999 and 2004. We conducted a phase II clinical trial using nimustine, carboplatin, vincristine, and IFN-β with radiotherapy for high-grade gliomas (KNOG study; ref. 19), and collected the major part of tumor specimens concomitantly with this trial. In most anaplastic oligodendroglioma cases, patients were treated by radiotherapy with chemotherapy of modified PCV regimen (procarbasine, nimustine, and vincristine). All cases were histologically diagnosed according to the WHO 2000 criteria at the primary hospital by a neuropathologist, and the original slides were reviewed centrally by the Kyoto University pathology unit for a final determination. To identify the diagnostic as well as prognostic genes responsible for differences in outcome between the two tumor classes, we focused on the histologically and clinically classic cases that received unanimous agreement by plural neuropathologists in histological diagnosis and followed the corresponding predicted clinical courses for their tumor type (Fig. 1A).

We examined known molecular prognostic factors, revealing that our anaplastic oligodendroglioma cases typically possessed a favorable molecular feature. Of 11 assessable anaplastic oligodendroglioma cases, 1p loss and combined loss of 1p and 19q were present in all 11 and 10 cases, respectively. On the other hand, of 13 assessable glioblastoma cases, 1p loss and combined loss of 1p and 19q were present in three and one case, respectively. MGMT promoter methylation was present in 5 of the 13 glioblastoma and 10 of the 11 anaplastic oligodendroglioma cases assessable. Interestingly, all 10 anaplastic oligodendroglioma cases with MGMT silencing simultaneously showed combined loss of 1p and 19q. p53 mutation was detected in 3 of the 16 glioblastoma assessable cases and none of all 12 anaplastic oligodendroglioma cases. EGFRvIII was present in only 1 glioblastoma case of 20 assessable cases, including 10 glioblastoma and 10 anaplastic oligodendroglioma cases. The clinical and molecular features of all 32 patients are summarized in Table 1.

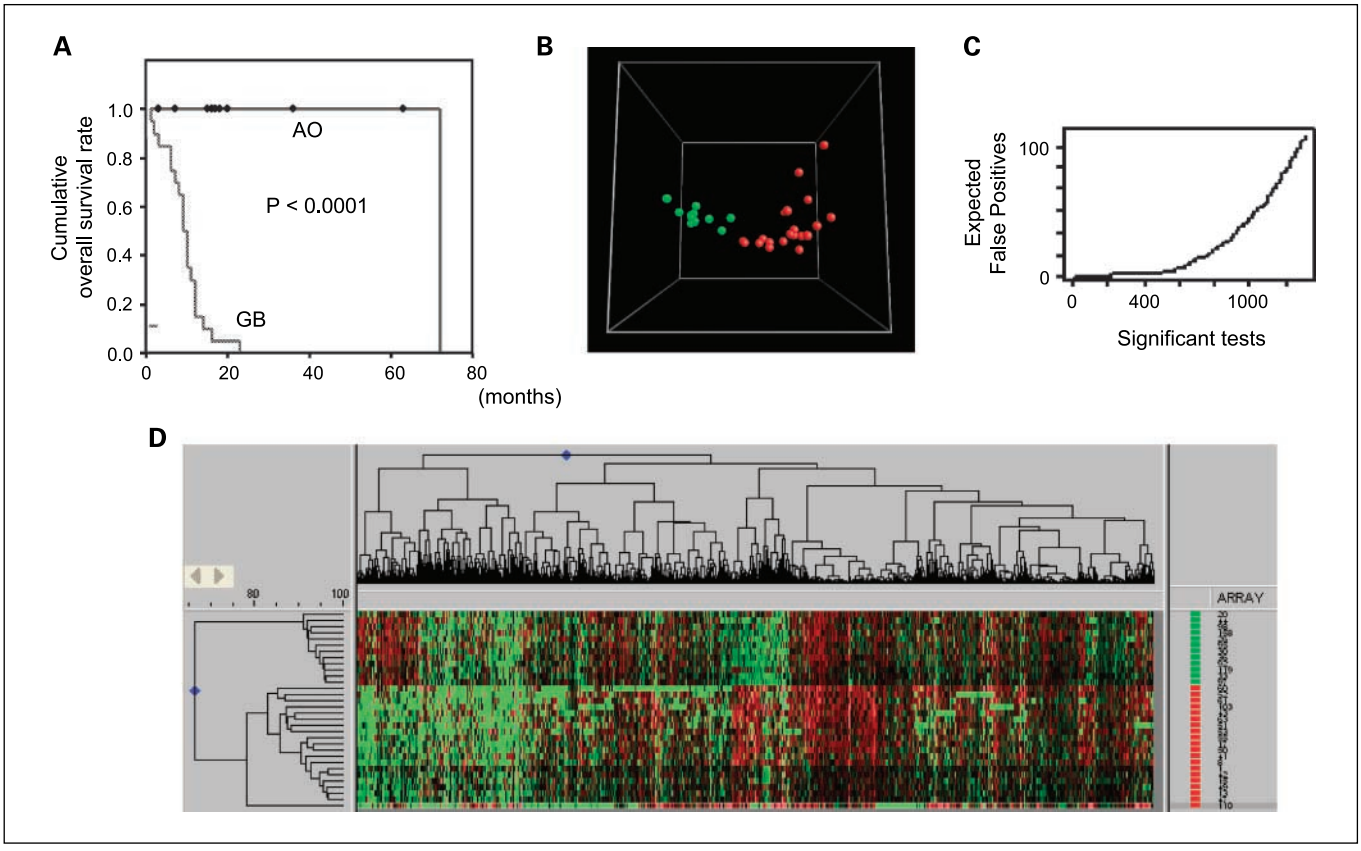

Fig. 1. *A,* Kaplan-Meier estimates of overall survival among 32 malignant gliomas [12 anaplastic oligodendrogliomas (*AO*) and 20 glioblastomas (*GB*)]. *P* value was calculated with the use of the log-rank test. *B,* principal component analysis of gene expression in 32 malignant gliomas. The variation in the expression levels of the 3,269 genes is reduced to a three-dimensional space. Each sphere represents each sample; green and red, anaplastic oligodendroglioma and glioblastoma, respectively. *C,* the expected number of false-positive genes versus the total number of significant genes given by the *q* values. *D,* unsupervised hierarchical clustering of 32 malignant gliomas using 3,269 genes. Genes (*horizontal axis*) and samples (*vertical axis*) were grouped by individual gene expression patterns. Green and red bars, anaplastic oligodendroglioma and glioblastoma, respectively.

Gene expression profiling. We measured the relative gene expression levels of 3,456 genes in the 32 gliomas using ATAC-PCR. Of the 3,456 genes, 3,269 genes were used for further analyses, excluding 187 genes that were missing in 20% or more of the cases.

First, we did an unsupervised analysis to obtain a general view of global gene expression signatures. Hierarchical cluster analysis of the 3,269 genes in all 32 gliomas showed that there were distinct patterns of expression for both anaplastic oligodendroglioma and glioblastoma (Fig. 1D). Principal component analysis also showed a clear separation between anaplastic oligodendroglioma and glioblastoma in reduced three-dimensional space (Fig. 1B). These results raise the possibility of classifying anaplastic oligodendroglioma and glioblastoma based on the expression levels of the diagnostic genes that they differentially express.

Then, we evaluated the statistical significance of the anaplastic oligodendroglioma/glioblastoma comparison for each gene by performing both P value and q value analyses. Of the 3,269 genes, 416 genes differed significantly between anaplastic oligodendroglioma and glioblastoma with a cutoff of P value = 0.001.The estimated number of false-positive genes was <2, with a q value of 0.00354 (Fig. 1C).

Next, we did a supervised analysis to construct a diagnostic system for classifying anaplastic oligodendroglioma and glioblastoma for practical use. We adopted a weighted voting algorithm with gene selection by signal-to-noise ratio ranking (17). This diagnostic system was confirmed using leave-one-out cross-validation, showing stable 100% (95% confidence interval, 89.4-100%) diagnostic accuracy in differentiating the test anaplastic oligodendroglioma and glioblastoma cases, using at least the 168 top-ranked genes (Supplementary Figure). Accordingly, we established the top 168 genes by signal-to-noise ratio ranking for all 32 cases as the classifier set. These genes were a subset of the 300 genes whose expression levels were significantly different between anaplastic oligodendroglioma and glioblastoma, with a rigid cutoff value of P = 0.0003, q = 0.0011.

Of the 168 selected classifier genes, the 87 genes showed higher expression in anaplastic oligodendroglioma samples (anaplastic oligodendroglioma classifier genes), including a group of genes involved in general neuronal function or neuronal differentiation (Table 2). On the other hand, the 81 genes with higher expression in glioblastoma samples (glioblastoma classifier genes) included a group of genes for which high expression was previously reported to be correlated

Table 1. Summary of the clinical and pathologic features in all 32 patients

Sample no.	Histology	Vital status	Survival (mo)*	Treatment	p53mut	EGFRvIIImut	MGMT methylation	1p LOH	19q LOH
1	GB	Dead	10	KNOG	-	-	NA	NA	NA
2	GB	Dead	2	RT + ACNU	NA	NA	NA	NA	NA
3	GB	Dead	12	KNOG	-	-	NA	NA	NA
4	GB	Dead	11	KNOG	+	NA	-	-	-
5	GB	Dead	3	RT + ACNU	-	-	+	-	-
6	GB	Dead	10	KNOG	-	NA	-	+	+
7	GB	Dead	23	KNOG	-	+	-	-	-
8	GB	Dead	12	KNOG	-	NA	-	-	+
9	GB	Dead	9	KNOG	+	-	+	-	-
10	GB	Dead	9	KNOG	-	NA	+	-	-
11	GB	Dead	6	KNOG	-	NA	+	+	-
12	GB	Dead	6	KNOG	NA	NA	-	-	+
13	GB	Dead	8	KNOG	+	NA	+	+	-
14	GB	Dead	16	KNOG	-	-	NA	NA	NA
15	GB	Dead	14	KNOG	-	-	NA	NA	NA
16	GB	Dead	10	KNOG	-	-	-	-	+
17	GB	Dead	7	KNOG	-	-	NA	NA	NA
18	GB	Dead	9	KNOG	-	-	-	-	+
19	GB	Dead	12	KNOG	NA	NA	-	-	-
20	GB	Dead	1	KNOG	NA	NA	NA	NA	NA
21	AO	Alive	7	PAV alone	-	NA	+	+	+
22	AO	Alive	3	RT + PAV	-	NA	+	+	+
23	AO	Dead	72	RT + PAV	-	-	+	+	+
24	AO	Alive	17	KNOG	-	-	NA	NA	NA
25	AO	Alive	63	RT + PAV	-	-	+	+	+
26	AO	Alive	20	RT + PAV	-	-	+	+	+
27	AO	Alive	18	RT + PAV	-	-	+	+	+
28	AO	Alive	18	KNOG	-	-	+	+	+
29	AO	Alive	18	RT + PAV	-	-	+	+	+
30	AO	Alive	36	RT + PAV	-	-	+	+	+
31	AO	Alive	16	RT + PAV	-	-	-	+	-
32	AO	Alive	15	KNOG	-	-	+	+	+

Abbreviations: LOH, loss of heterozygosity; AO, anaplastic oligodendroglioma; GB glioblastoma; KNOG, nimustine, carboplatin, vincristine, and IFN-β with radiotherapy; PAV, procarbazine, nimustine, vincristine; RT, radiotherapy; ACNU, nimustine; NA, not analyzed.
*Survival from date of operation given for all patients. For living patients, survival was given to time of last follow-up.

with the malignant character of glioblastoma (Table 3). Functional group analysis revealed that the biological process in which classifier genes involved were distinctively different between two tumor classes. Significantly more glioblastoma classifier genes were associated with cell motility and cell adhesion, whereas prominently more anaplastic oligodendroglioma classifier genes were associated with neuron-related functions such as neuron fate commitment, nervous system development, and synaptic activity (Table 4). Analysis of chromosomal positions of classifier genes revealed that there were fewer anaplastic oligodendroglioma classifier genes on 1p and 19q than glioblastoma classifier genes, reflecting the loss of 1p and 19q in most anaplastic oligodendroglioma cases (Tables 2 and 3).

Then, to validate the diagnostic accuracy of our algorithm in an independent test set, we applied our classifier genes to a MGH data set of 50 malignant gliomas from a previous microarray study (20). The 50 gliomas consisted of 26 classic gliomas that were diagnosed in unanimous agreement by multiple neuropathologists and 24 nonclassic gliomas for which the histological diagnoses were controversial. The expression levels of 67 genes of our 168 genes were available, so we did molecular diagnosis on these 50 gliomas using the expression data of these 67 genes. From these calculations, there was an obvious tendency for the calculated PS of the glioblastoma cases to be higher than those of the anaplastic oligodendroglioma cases (Fig. 2A). When the cutoff value was set to zero, our molecular diagnoses were completely consistent with the histological diagnoses for the 14 cases of classic glioblastoma. Our diagnoses were also consistent for three of the seven cases of classic anaplastic oligodendroglioma. Among the seven classic anaplastic oligodendrogliomas, two turned out to have overall survival periods of less than 1 year. Interestingly, these two dismal cases were both classified as glioblastoma by our classifier genes. In total, our molecular diagnoses agreed with those of the original article for 28 of 29 of the nonclassic malignant glioma cases (96.6%). Furthermore, when compared with traditional histopathologic diagnosis, our molecular classifier genes showed significantly greater ability to accurately predict the survival time for all 50 glioma patients (Fig. 2B and C). In addition, among the 28 cases of histologically diagnosed glioblastoma, the patients with a lower PS tended to have prolonged survival. Dividing the glioblastoma cases into two groups with a cutoff value of 0.4 simply set by the break on scatter plots among the classic glioblastomas, the survival rate of the patients with a lower PS was significantly higher than that of patients with a higher PS (Fig. 2D).

Finally, we applied the classifier genes in the MGH study to our data set. Among the genes used in the MGH study, we found 19 genes in our data matrix. As in the MGH study, we did classification by *K*-nearest neighbor with the 19 genes: 30 of 32 cases (94% accuracy) were accurately predicted.

Discussion

Classification of gliomas according to their molecular features is expected to reflect their clinical behavior or outcome. In this study, we focused on the clinicopathologically classic anaplastic oligodendroglioma and glioblastoma cases to capture the intrinsic biological difference between two tumor classes. We documented the striking differences in global gene expression signature between two tumor classes and showed that these differences were actually predictive of the future clinical course. We constructed a molecular diagnostic system capable of discriminating anaplastic oligodendroglioma from glioblastoma based on ATAC-PCR gene expression profiling data. Our system displayed clinical utility and provided reproducible prognostic ability as confirmed by testing on a public microarray-based data set.

Interestingly, the selected classifier genes for each class possessed a distinctive feature in functional aspects. Among the classifier genes whose expression levels were higher in anaplastic oligodendroglioma samples, many genes are implicated in general neuronal function or in neural development. In particular, functional group analysis revealed that the genes associated with neuron fate commitment were most enriched in the anaplastic oligodendroglioma classifier genes. Recent study revealed a close correlation between the stage in neural development and the prognostic classes among high-grade gliomas. Similar to our finding, they showed that strong expression of markers of committed neuronal lineage was the characteristic feature of a good prognosis group (21). These results stressed the prognostic significance of the expression of neuronal lineage markers but also might offer clues for understanding the genesis of anaplastic oligodendroglioma. The neuronal feature in classic anaplastic oligodendrogliomas may reflect the cell they originated from. The previous studies showed that most of the genes showing distinctive expression in oligodendroglial tumors with allelic loss of chromosome 1p had neuron-related functions (22, 23). Of the genes they indicated as diagnostic markers for oligodendroglial tumors with 1p loss, *SNCB*, *INA*, *L1CAM*, and *RIMS2* were also included in our classifier gene set.

In addition to such a neural character, some anaplastic oligodendroglioma classifier genes have been reported to be expressed in cells of the oligodendroglial lineage. Olig-1 and Olig-2 are both broadly expressed throughout oligodendrocyte development (24). Although previous studies revealed that Olig genes are not necessarily specific markers for oligodendroglial tumors (25, 26), our finding that expression of Olig-1 and Olig-2 was significantly lower in glioblastoma samples than in anaplastic oligodendroglioma samples indicates its utility in discriminating anaplastic oligodendroglioma from glioblastoma. Another pair of transcription factors, Sox-4 and Sox-8, which were also reported to be expressed in cells of the oligodendrocyte lineage, functioned as classifier genes for anaplastic oligodendroglioma and glioblastoma (27, 28). These results suggest that anaplastic oligodendroglioma shares some of the characteristic gene expression patterns of oligodendrocyte progenitors, and that these oligodendrocyte lineage genes, when used as a set, might act as a powerful diagnostic marker for anaplastic oligodendroglioma.

Conversely, the classifier genes up-regulated in glioblastoma samples included a group of genes that are involved in the tumor invasion process, one of the hallmark malignant features of glioblastoma. The functional group analysis statistically endorsed the result, demonstrating that the genes associated with cell motility and adhesion, which are the main biological processes of tumor invasion, were significantly enriched among glioblastoma classifier genes. The previous microarray study investigated the genes involved in glioma cell motility (29). Of genes up-regulated with increased glioma cell motility,

Table 2. List of genes showing higher expression in anaplastic oligodendrogliomas

No	STNR	GS no.	Gene symbol	Genomic location	Genbank accession no.	Definition	General neuronal function or neuronal differentiation
1	2.136	GS14040	*INA*	10q24.33	NM_032727	*Homo sapiens* internexin neuronal intermediate filament protein, α (INA), mRNA	*
2	1.964	GS1818	*NDRG2*	14q11.2	NM_201538	*Homo sapiens* NDRG family member 2 (NDRG2), transcript variant 5, mRNA	*
3	1.926	—	*SOX4*	6p22.3	NM_003107	*Homo sapiens* SRY (sex determining region Y)-box 4 (SOX4), mRNA	*
4	1.864	GS13667	*BRSK2*	11p15.5	NM_003957	*Homo sapiens* BR serine/threonine kinase 2 (BRSK2), mRNA	*
5	1.853	GS13989	*TUB*	11p15.5	NM_003320	*Homo sapiens* tubby homologue (mouse; TUB), transcript variant 1, mRNA	*
6	1.848	GS14085	*GDAP1L1*	20q12	NM_024034	*Homo sapiens* ganglioside-induced differentiation-associated protein 1-like 1 (GDAP1L1), mRNA	*
7	1.815	GS13275	*RPIP8*	17q21.31	AB209802	*Homo sapiens* mRNA for RaP2 interacting protein 8 variant protein	*
8	1.808	GS12750	*ACTL6B*	7q22	NM_016188	*Homo sapiens* actin-like 6B (ACTL6B), mRNA	*
9	1.775	GS12811	*SCG3*	15q21	NM_013243	*Homo sapiens* secretogranin III (SCG3), mRNA	*
10	1.752	GS13065	*ATP1A3*	19q13.31	NM_152296	*Homo sapiens* ATPase, Na^+/K^+ transporting, α3 polypeptide (ATP1A3), mRNA	*
11	1.747	GS14014	*SPTBN2*	11q13	NM_006946	*Homo sapiens* spectrin, β, nonerythrocytic 2 (SPTBN2), mRNA	*
12	1.746	GS6687	*CHGB*	20pter-p12	NM_001819	*Homo sapiens* chromogranin B (secretogranin 1; CHGB), mRNA	*
13	1.714	GS13304	*CA10*	17q21	NM_020178	*Homo sapiens* carbonic anhydrase X (CA10), mRNA	
14	1.697	GS4519	*ALCAM*	3q13.1	NM_001627	*Homo sapiens* activated leukocyte cell adhesion molecule (ALCAM), mRNA	*
15	1.606	GS13651	*PEN11B*	11p15.5	AF020089	*Homo sapiens* PEN11B mRNA, complete cds	*
16	1.593	GS4155	*SYN1*	Xp11.23	M58378	Human synapsin I (SYN1) gene, exon 13	*
17	1.577	GS12571	*DNAJC12*	10q22.1	NM_021800	*Homo sapiens* DnaJ (Hsp40) homologue, subfamily C, member 12 (DNAJC12), transcript variant 1, mRNA	
18	1.543	GS12884	*CPLX2*	5q35.2	NM_001008220	*Homo sapiens* complexin 2 (CPLX2), transcript variant 2, mRNA	*
19	1.538	—	*RIMS2*	8q22.3	NM_014677	*Homo sapiens* regulating synaptic membrane exocytosis 2 (RIMS2),mRNA	*
20	1.524	GS13961	*PHYHIPL*	10q11	NM_032439	*Homo sapiens* phytanoyl-CoA hydroxylase interacting protein-like (PHYHIPL), mRNA	
21	1.465	GS12771	*SYP*	Xp11.23-p11.22	NM_003179	*Homo sapiens* synaptophysin (SYP), mRNA	*
22	1.458	GS12839	*HMP19*	5q35.2	NM_015980	*Homo sapiens* HMP19 protein (HMP19), mRNA	*

(*Continued on the following page*)

Table 2. List of genes showing higher expression in anaplastic oligodendrogliomas (Cont'd)

No	STNR	GS no.	Gene symbol	Genomic location	Genbank accession no.	Definition	General neuronal function or neuronal differentiation
23	1.448	GS14072	*KCNQ2*	20q13.3	NM_004518	*Homo sapiens* potassium voltage-gated channel, KQT-like subfamily, member 2 (KCNQ2), transcript variant 3, mRNA	*
24	1.438	GS11751	*EST*	—	—	—	
25	1.414	GS13137	*ARHGDIG*	16p13.3	NM_001176	*Homo sapiens* Rho GDP dissociation inhibitor (GDI) γ (ARHGDIG), mRNA	*
26	1.385	GS13019	*HES6*	2q37.3	NM_018645	*Homo sapiens* hairy and enhancer of split 6 (*Drosophila*; HES6), mRNA	*
27	1.382	GS13762	*KIAA0927 protein*	22q12.1	AB023144	*Homo sapiens* mRNA for KIAA0927 protein, partial cds	
28	1.344	GS7227	*DKFZp434J212*	1pter-q31.3	BC078676	*Homo sapiens* kinesin family member 21B, mRNA (cDNA clone IMAGE:5141761)	
29	1.323	GS13181	*TNK2*	3q29	NM_001010938	*Homo sapiens* tyrosine kinase, nonreceptor, 2 (TNK2), transcript variant 2, mRNA	*
30	1.320	GS13046	*Ells1*	7p15.1	NM_152793	Hypothetical protein FLJ39214	
31	1.309	—	*ABCC8*	11p15.1	NM_000352	*Homo sapiens* ATP-binding cassette, subfamily C (CFTR/MRP), member8 (ABCC8), mRNA	
32	1.284	GS14148	*DKFZp434H205*	—	AL117636	*Homo sapiens* mRNA; cDNA DKFZp434H205 (from clone DKFZp434H205)	
33	1.279	GS12813	*ATP6V1G2*	6p21.3	NM_138282	ATPase, H^+ transporting, lysosomal, V1 subunit	
34	1.278	GS11593	*APBB1*	11p15	NM_001164	*Homo sapiens* amyloid β (A4) precursor protein-binding, family B, member 1 (Fe65; APBB1), transcript variant 1, mRNA	*
35	1.273	GS13340	*PKNOX2*	—	NM_022062	*Homo sapiens* PBX/knotted 1 homeobox 2 (PKNOX2), mRNA	
36	1.267	GS10002	*ALDOC*	17cen-q12	NM_005165	*Homo sapiens* aldolase C, fructose-bisphosphate (ALDOC), mRNA	*
37	1.264	GS13880	*JPH4*	14q11	NM_032452	*Homo sapiens* junctophilin 4 (JPH4), mRNA	*
38	1.253	GS1752	*ABAT*	16p13.2	NM_000663	*Homo sapiens* 4-aminobutyrate aminotransferase (ABAT), nuclear gene encoding mitochondrial protein, transcript variant 2, mRNA	*
39	1.252	GS13457	*clone24425*	—	AF070565	*Homo sapiens* clone 24425 mRNA sequence	
40	1.243	GS3816	*NFIX*	19p13.3	NM_002501	*Homo sapiens* nuclear factor I/X (CCAAT-binding transcription factor; NFIX), mRNA	
41	1.232	GS11850	*BC024752*	16q22.1	BC024752	*Homo sapiens* cDNA clone IMAGE:5123182, partial cds	
42	1.223	—	*SNCB*	5q35	NM_001001502	*Homo sapiens* synuclein, β (SNCB), transcript variant 1, mRNA	*
43	1.219	GS13487	*OLIG1*	21q22.11	NM_138983	*Homo sapiens* oligodendrocyte transcription factor 1 (OLIG1), mRNA	
44	1.214	GS14208	*BC041405*	—	BC041405	*Homo sapiens*, clone IMAGE:5284125, mRNA	

(*Continued on the following page*)

Table 2. List of genes showing higher expression in anaplastic oligodendrogliomas (Cont'd)

No	STNR	GS no.	Gene symbol	Genomic location	Genbank accession no.	Definition	General neuronal function or neuronal differentiation
45	1.209	GS12762	*ATCAY*	19p13.3	NM_033064	*Homo sapiens* ataxia, cerebellar, Cayman type (caytaxin; ATCAY), mRNA	*
46	1.207	GS6693	*KIAA0471*	1q24	AB007940	*Homo sapiens* mRNA for KIAA0471 protein, partial cds	
47	1.203	—	*SOX8*	16p13.3	NM_014587	*Homo sapiens* SRY (sex determining region Y)-box 8 (SOX8), mRNA	
48	1.201	GS14478	*L1CAM*	Xq28	NM_000425	*Homo sapiens* L1 cell adhesion molecule (L1CAM), transcript variant 1, mRNA	*
49	1.198	—	*OLIG1*	21q22.11	NM_138983	*Homo sapiens* oligodendrocyte transcription factor 1 (OLIG1), mRNA	
50	1.195	GS14103	*BC094805*	—	BC094805	*Homo sapiens* cDNA clone IMAGE:5015789	
51	1.168	GS685	*SLC22A17*	14q11.2	NM_020372	*Homo sapiens* solute carrier family 22 (organic cation transporter), member 17 (SLC22A17), transcript variant 1, mRNA	
52	1.160	GS14283	*BC040444*	17q21.1	BC040444	*Homo sapiens* cDNA clone IMAGE:5770508	
53	1.157	GS12682	*OLIG2*	21q22.11	NM_005806	*Homo sapiens* oligodendrocyte lineage transcription factor 2 (OLIG2), mRNA	
54	1.152	GS14490	*EST*	8q21.2	AF070623	*Homo sapiens* clone 24468 mRNA sequence	
55	1.149	GS13380	*KIAA1337*	1p36.22	AB037758	*Homo sapiens* mRNA for KIAA1337 protein, partial cds	
56	1.149	GS12805	*EST*	—	—	—	
57	1.148	—	*MYCN*	2p24.1	NM_005378	*Homo sapiens* v-myc myelocytomatosis viral related oncogene, neuroblastoma derived (avian; MYCN), mRNA	
58	1.146	GS643	*RPL15*	3p24.2	NM_002948	*Homo sapiens* ribosomal protein L15 (RPL15), mRNA	
59	1.141	GS14691	*CKLFSF5*	—	NM_181618	*Homo sapiens* chemokine-like factor superfamily 5 (CKLFSF5), transcript variant 2, mRNA	
60	1.131	GS14254	*FAM19A5*	22q13.32	NM_015381	*Homo sapiens* family with sequence similarity 19 (chemokine (C-C motif)-like), member A5 (FAM19A5), mRNA	*
61	1.128	GS13133	*AB056341*	—	AB056341	*Macaca fascicularis* brain cDNA, clone:QflA-15195	
62	1.124	—	*OMG*	17q11.2	NM_002544	*Homo sapiens* oligodendrocyte myelin glycoprotein (OMG), mRNA	
63	1.118	GS13976	*RIPX*	4q13.3	NM_014961	*Homo sapiens* rap2 interacting protein x (RIPX), mRNA	
64	1.116	GS11781	*DKFZp761P2314*	—	AL834342	*Homo sapiens* mRNA; cDNA DKFZp761P2314 (from clone DKFZp761P2314)	
65	1.107	GS12728	*BCAN*	1q31	NM_021948	*Homo sapiens* brevican (BCAN), mRNA	*
66	1.103	GS13198	*PPP1R3F*	Xp11.23	NM_033215	*Homo sapiens* protein phosphatase 1, regulatory (inhibitor) subunit 3F (PPP1R3F), mRNA	

(*Continued on the following page*)

Table 2. List of genes showing higher expression in anaplastic oligodendrogliomas (Cont'd)

No	STNR	GS no.	Gene symbol	Genomic location	Genbank accession no.	Definition	General neuronal function or neuronal differentiation
67	1.100	GS12906	*STXBP1*	9q34.1	NM_003165	*Homo sapiens* syntaxin binding protein 1 (STXBP1), mRNA	*
68	1.090	GS14082	*ELAVL3*	19p13.2	NM_032281	*Homo sapiens* ELAV (embryonic lethal, abnormal vision, *Drosophila*)-like 3 (Hu antigen C; ELAVL3), transcript variant 2, mRNA	*
69	1.083	GS13726	*RNF41*	12q13.2	NM_194359	*Homo sapiens* ring finger protein 41 (RNF41), transcript variant 3, mRNA	
70	1.083	GS12702	*KIAA1128*	10q23.1	NM_018999	*Homo sapiens* KIAA1128 (KIAA1128), mRNA	
71	1.080	GS13482	*EST*	—	—	—	
72	1.077	GS14338	*CNTFR*	9p13	NM_147164	*Homo sapiens* ciliary neurotrophic factor receptor (CNTFR), mRNA	*
73	1.074	GS12998	*CAMK2N2*	3q27.1	NM_033259	*Homo sapiens* calcium/ calmodulin-dependent protein kinase II inhibitor 2 (CAMK2N2), mRNA	*
74	1.074	GS14540	*KIAA0527*	3p22.3	AB011099	*Homo sapiens* mRNA for KIAA0527 protein, partial cds	
75	1.061	GS13729	*FLJ30046*	13q22.3	NM_144595	*Homo sapiens* hypothetical protein FLJ30046 (FLJ30046), mRNA	
76	1.059	GS7935	*FXYD6*	11q23.3	NM_022003	*Homo sapiens* FXYD domain containing ion transport regulator 6 (FXYD6), mRNA	
77	1.052	GS13356	*PDZK4*	Xq28	NM_032512	*Homo sapiens* PDZ domain containing 4 (PDZK4), mRNA	
78	1.052	GS11619	*SLC6A1*	3p25-p24	NM_003042	*Homo sapiens* solute carrier family 6 (neurotransmitter transporter, GABA), member 1 (SLC6A1), mRNA	
79	1.049	GS14578	*DKFZp761E1116*	-	AL390131	*Homo sapiens* mRNA; cDNA DKFZp761E1116 (from clone DKFZp761E1116)	
80	1.039	GS6318	*HR*	8p21.2	NM_005144	*Homo sapiens* hairless homologue (mouse; HR), mRNA	
81	1.035	GS3177	*MGC40157*	17p11.2	NM_152350	Hypothetical protein MGC40157	
82	1.032	GS14588	*GRIA2*	4q32-q33	NM_000826	*Homo sapiens* glutamate receptor, ionotropic, AMPA 2 (GRIA2), mRNA	*
83	1.029	GS191	*NACA*	12q23-q24.1	NM_005594	*Homo sapiens* nascent-polypeptide-associated complex α polypeptide (NACA), mRNA	
84	1.021	GS2746	*EST*	—	—	—	
85	1.019	GS4380	*IDI1*	10p15.3	NM_004508	*Homo sapiens* isopentenyl-diphosphate δ isomerase (IDI1), mRNA	
86	1.008	GS13230	*FLJ39293*	5p15.31	AK096612	*Homo sapiens* cDNA FLJ39293 fis, clone OCBBF2012678	
87	1.005	—	*ACCN2*	12q12	NM_020039	*Homo sapiens* amiloride-sensitive cation channel 2, neuronal (ACCN2), transcript variant 1, mRNA	*

NOTE: The genes are listed in ascending order determined by the absolute value of signal-to-noise ratio. GS number is the in-house gene identification number.

*The genes marked with an asterisk were reported to be involved in general neuronal function or neuronal differentiation.

Table 3. List of genes showing higher expression in glioblastomas

No.	STNR	GS no.	Gene symbol	Genomic location	Genbank accession no.	Definition
1	2.209	GS1683	*IFITM3*	11p15.5	NM_021034	*Homo sapiens* IFN induced transmembrane protein 3 (1-8U; IFITM3), mRNA
2	1.998	—	*TNC*	9q33	NM_002160	*Homo sapiens* tenascin C (hexabrachion; TNC), mRNA
3	1.891	GS475	*LDHA*	11p15.4	NM_005566	*Homo sapiens* lactate dehydrogenase A (LDHA), mRNA
4	1.831	—	*VIM*	10p13	NM_003380	*Homo sapiens* vimentin (VIM), mRNA
5	1.816	GS4232	*TNC*	9q33	NM_002160	Tenascin C (hexabrachion)
6	1.751	GS2482	*IGFBP2*	2q33-q34	NM_000597	*Homo sapiens* insulin-like growth factor binding protein 2, 36 kDa (IGFBP2), mRNA
7	1.663	GS208	*IFI30*	19p13.1	NM_006332	*Homo sapiens* IFN, γ-inducible protein 30 (IFI30), mRNA
8	1.654	GS7306	*RHOC*	1p13.1	NM_175744	*Homo sapiens* ras homologue gene family, member C (RHOC), mRNA
9	1.601	GS10556	*MSN*	Xq11.2-q12	NM_002444	*Homo sapiens* moesin (MSN), mRNA
10	1.571	GS12786	*LAMB2*	3p21	NM_002292	*Homo sapiens* laminin, β_2 (laminin S; LAMB2), mRNA
11	1.567	GS3926	*MYL6*	12q13.2	NM_079423	*Homo sapiens* myosin, light polypeptide 6, alkali, smooth muscle and nonmuscle (MYL6), transcript variant 2, mRNA
12	1.563	—	*YKL40*	1q32.1	NM_001276	*Homo sapiens* chitinase 3-like 1 (cartilage glycoprotein-39; CHI3L1), mRNA
13	1.537	GS4923	*TIMP1*	Xp11.3-p11.23	NM_003254	*Homo sapiens* tissue inhibitor of metalloproteinase 1 (erythroid potentiating activity, collagenase inhibitor; TIMP1), mRNA
14	1.511	GS2427	*CD14*	5q22-q32;5q31.1	NM_000591	*Homo sapiens* CD14 antigen (CD14), mRNA
15	1.498	GS1769	*ENO1*	1p36.3-p36.2	NM_001428	*Homo sapiens* enolase 1, (α; ENO1), mRNA
16	1.495	GS4332	*RPN2*	20q12-q13.1	NM_002951	*Homo sapiens* ribophorin II (RPN2), mRNA
17	1.485	GS4168	*TAGLN2*	1q21-q25	NM_003564	*Homo sapiens* transgelin 2 (TAGLN2), mRNA
18	1.475	GS13490	*DKFZp564P143*	—	AL049298	*Homo sapiens* mRNA; cDNA DKFZp564P143 (from clone DKFZp564P143)
19	1.413	GS4080	*PSMD8*	19q13.2	NM_002812	*Homo sapiens* proteasome (prosome, macropain) 26S subunit, non-ATPase, 8 (PSMD8), mRNA
20	1.410	GS421	*TMSB4X*	Xq21.3-q22	NM_021109	*Homo sapiens* thymosin, β 4, X-linked (TMSB4X), mRNA
21	1.404	GS3240	*CD63*	12q12-q13	NM_001780	*Homo sapiens* CD63 antigen (melanoma 1 antigen; CD63), mRNA
22	1.390	GS3483	*ZYX*	7q32	NM_001010972	*Homo sapiens* zyxin (ZYX), mRNA
23	1.347	GS3909	*VMP1*	17q23.1	NM_030938	Hypothetical protein DKFZp566I133, Alt-splicing
24	1.342	GS9541	*ARPC1B*	7q22.1	NM_005720	*Homo sapiens* actin related protein 2/3 complex, subunit 1B, 41 kDa (ARPC1B), mRNA
25	1.323	GS139	*FTL*	19q13.3-q13.4	NM_000146	*Homo sapiens* ferritin, light polypeptide (FTL), mRNA
26	1.295	GS4210	*NPC2*	14q24.3	NM_006432	*Homo sapiens* Niemann-Pick disease, type C2 (NPC2), mRNA
27	1.294	—	*TYROBP*	19q13.1	NM_003332	*Homo sapiens* TYRO protein tyrosine kinase binding protein (TYROBP), transcript variant 1, mRNA
28	1.285	GS7820	*CD99*	Xp22.32; Yp11.3	NM_002414	*Homo sapiens* CD99 antigen (CD99), mRNA
29	1.282	—	*TMSB10*	2p11.2	NM_021103	*Homo sapiens* thymosin, β 10 (TMSB10), mRNA
30	1.274	GS1756	*LR8*	7q36.1	NM_014020	*Homo sapiens* LR8 protein (LR8), mRNA
31	1.257	GS6132	*PLEKHA4*	19q13.33	NM_020904	*Homo sapiens* pleckstrin homology domain containing, family A (phosphoinositide binding specific) member 4 (PLEKHA4), mRNA
32	1.257	GS1458	*MRCL3*	18p11.31	NM_006471	*Homo sapiens* myosin regulatory light chain MRCL3 (MRCL3), mRNA
33	1.254	—	*FN14*	16p13.3	NM_016639	*Homo sapiens* tumor necrosis factor receptor superfamily, member 12A (TNFRSF12A), mRNA

(*Continued on the following page*)

Table 3. List of genes showing higher expression in glioblastomas (Cont'd)

No.	STNR	GS no.	Gene symbol	Genomic location	Genbank accession no.	Definition
34	1.251	GS242	*S100A10*	1q21	NM_002966	*Homo sapiens* S100 calcium binding protein A10 (Annexin II ligand, calpactin I, light polypeptide (p11); S100A10), mRNA
35	1.251	GS1890	*LGALS1*	22q13.1	NM_002305	*Homo sapiens* lectin, galactoside-binding, soluble, 1 (galectin 1; LGALS1), mRNA
36	1.241	GS315	*SFRS11*	1p31	NM_004768	*Homo sapiens* splicing factor, arginine/serine-rich 11 (SFRS11), mRNA
37	1.237	GS2223	*SOD2*	6q25.3	NM_001024466	*Homo sapiens* superoxide dismutase 2, mitochondrial (SOD2), nuclear gene encoding mitochondrial protein, transcript variant 3, mRNA
38	1.234	—	*A2M*	12p13.3-p12.3	NM_000014	*Homo sapiens* α-2-macroglobulin (A2M), mRNA
39	1.233	GS846	*CD74*	5q32	NM_004355	*Homo sapiens* CD74 antigen (invariant polypeptide of MHC, class II antigen-associated; CD74), mRNA
40	1.226	GS9792	*ATP6V0B*	1p32.3	NM_004047	*Homo sapiens* ATPase, H^+ transporting, lysosomal 21 kDa, V0 subunit c″ (ATP6V0B), mRNA
41	1.218	GS1071	*DKFZp686L01105*	—	BX647603	*Homo sapiens* mRNA; cDNA DKFZp686L01105 (from clone DKFZp686L01105)
42	1.215	GS3760	*AEBP1*	7p13	NM_001129	*Homo sapiens* AE binding protein 1 (AEBP1), mRNA
43	1.201	—	*FLNA*	Xq28	NM_001456	*Homo sapiens* filamin A, α (actin binding protein 280; FLNA), mRNA
44	1.200	GS4681	*CLIC4*	1p36.11	NM_013943	*Homo sapiens* chloride intracellular channel 4 (CLIC4), mRNA
45	1.186	GS6844	*GPI*	19q13.1	NM_000175	*Homo sapiens* glucose phosphate isomerase (GPI), mRNA
46	1.168	GS11909	*TCTE1L*	Xp21	NM_006520	*Homo sapiens* t-complex-associated-testis-expressed 1-like (TCTE1L), mRNA
47	1.159	—	*MMP14*	14q11-q12	NM_004995	*Homo sapiens* matrix metallopeptidase 14 (membrane-inserted; MMP14), mRNA
48	1.147	—	*ANX1*	9q12-q21.2; 9q12-q21.2	NM_000700	*Homo sapiens* Annexin A1 (ANXA1), mRNA
49	1.134	GS1771	*ATPIF1*	—	NM_178191	*Homo sapiens* ATPase inhibitory factor 1 (ATPIF1), nuclear gene encoding mitochondrial protein, transcript variant 3, mRNA
50	1.133	GS1089	*ARPC3*	12q24.11	NM_005719	*Homo sapiens* actin related protein 2/3 complex, subunit 3, 21 kDa (ARPC3), mRNA
51	1.128	GS464	*SPI1*	11p11.2	NM_003120	*Homo sapiens* spleen focus forming virus (SFFV) proviral integration oncogene spi1 (SPI1), mRNA
52	1.127	GS2882	*SERF2*	15q15.3	NM_001018108	*Homo sapiens* small EDRK-rich factor 2 (SERF2), mRNA
53	1.118	GS214	*TAPBP*	6p21.3	NM_003190	*Homo sapiens* TAP binding protein (tapasin; TAPBP), transcript variant 1, mRNA
54	1.118	GS7407	*TRIP6*	7q22	NM_003302	*Homo sapiens* thyroid hormone receptor interactor 6 (TRIP6), mRNA
55	1.114	GS8756	*GATM*	15q21.1	NM_001482	*Homo sapiens* glycine amidinotransferase (L-arginine:glycine amidinotransferase; GATM), mRNA
56	1.108	—	*ALOX5AP*	13q12	NM_001629	*Homo sapiens* arachidonate 5-lipoxygenase-activating protein (ALOX5AP), mRNA
57	1.097	—	*CD44*	11p13	NM_000610	*Homo sapiens* CD44 antigen (homing function and Indian blood group system; CD44), transcript variant 1, mRNA
58	1.096	GS13416	*CAPNS1*	19q13.12	NM_001003962	*Homo sapiens* calpain, small subunit 1 (CAPNS1), transcript variant 2, mRNA
59	1.091	GS13941	*MEP50*	1p13.2	NM_024102	*Homo sapiens* methylosome protein 50 (MEP50), mRNA

(*Continued on the following page*)

Table 3. List of genes showing higher expression in glioblastomas (Cont'd)

No.	STNR	GS no.	Gene symbol	Genomic location	Genbank accession no.	Definition
60	1.091	GS13486	*CGI-38*	16q22.1	NM_015964	*Homo sapiens* brain-specific protein (CGI-38), mRNA
61	1.090	GS7265	*P8*	16p11.2	NM_012385	*Homo sapiens* p8 protein (candidate of metastasis 1; P8), mRNA
62	1.081	GS6741	*PKIG*	20q12-q13.1	NM_181805	*Homo sapiens* protein kinase (cAMP-dependent, catalytic) inhibitor γ (PKIG), transcript variant 1, mRNA
63	1.078	GS946	*LAPTM4A*	2p24.1	NM_014713	*Homo sapiens* lysosomal-associated protein transmembrane 4α (LAPTM4A), mRNA
64	1.069	GS4571	*SDC4*	20q12	NM_002999	*Homo sapiens* syndecan 4 (amphiglycan, ryudocan; SDC4), mRNA
65	1.066	GS4202	*NDUFA3*	19q13.42	NM_004542	*Homo sapiens* NADH dehydrogenase (ubiquinone) 1α subcomplex, 3, 9 kDa (NDUFA3), mRNA
66	1.065	—	*ITGA5*	12q11-q13	NM_002205	*Homo sapiens* integrin, α 5 (fibronectin receptor, αpolypeptide; ITGA5), mRNA
67	1.063	GS2065	*TMED9*	5q35.3	NM_017510	*Homo sapiens* transmembrane emp24 protein transport domain containing 9 (TMED9), mRNA
68	1.063	GS13922	*F13A1*	6p25.3-p24.3	NM_000129	*Homo sapiens* coagulation factor XIII, A1 polypeptide (F13A1), mRNA
69	1.061	GS13564	*GPSM3*	6p21.3	NM_022107	*Homo sapiens* G-protein signaling modulator 3 (AGS3-like, *C. elegans*; GPSM3), mRNA
70	1.060	—	*MCP1*	17q11.2-q12	NM_002982	*Homo sapiens* chemokine (C-C motif) ligand 2 (CCL2), mRNA
71	1.060	GS2782	*CLIC1*	6p22.1-p21.2	NM_001288	*Homo sapiens* chloride intracellular channel 1 (CLIC1), mRNA
72	1.059	GS3317	*RABAC1*	19q13.2	NM_006423	*Homo sapiens* Rab acceptor 1 (prenylated; RABAC1), mRNA
73	1.058	GS13503	*UPP1*	7p12.3	NM_181597	*Homo sapiens* uridine phosphorylase 1 (UPP1), transcript variant 2, mRNA
74	1.050	—	*PLAUR*	19q13	NM_001005376	*Homo sapiens* plasminogen activator, urokinase receptor (PLAUR), transcript variant 2, mRNA
75	1.048	GS220	*PSMC2*	7q22.1-q22.3	NM_002803	*Homo sapiens* proteasome (prosome, macropain) 26S subunit, ATPase, 2 (PSMC2), mRNA
76	1.046	GS1833	*HSPA5*	9q33-q34.1	NM_005347	*Homo sapiens* heat shock 70 kDa protein 5 (glucose-regulated protein, 78 kDa; HSPA5), mRNA
77	1.042	GS8061	*AXL*	19q13.1	NM_001699	*Homo sapiens* AXL receptor tyrosine kinase (AXL), transcript variant 2, mRNA
78	1.038	GS19	*PPP1A*	11q13	NM_002708	Protein phosphatase 1, catalytic subunit, α isoform
79	1.034	GS3823	*CTSD*	11p15.5	NM_001909	*Homo sapiens* cathepsin D (lysosomal aspartyl protease; CTSD), mRNA
80	1.014	—	*PAI1*	7q21.3-q22	NM_000602	*Homo sapiens* serpin peptidase inhibitor, clade E (nexin, plasminogen activator inhibitor type 1), member 1 (SERPINE1), mRNA
81	1.006	GS2570	*UBE2D2*	5q31.2	NM_181838	*Homo sapiens* ubiquitin-conjugating enzyme E2D 2 (UBC4/5 homologue, yeast; UBE2D2), transcript variant 2, mRNA

Abbreviation: STNR, signal-to-noise ratio.

Tenascin-C, CD44, Fn14, PAI-1, Annexin1, and *Moesin* were also included in our gene set. Invasion of glioma cells into adjacent brain tissue is dependent on their interaction with the extracellular matrix. Extracellular matrix components and cell surface receptors such as Tenascin-C, CD44, and Fn14 play a major role in regulating cell migration, and have been suggested as the principle mediators of the glioma invasion process (30–32). Urokinase plasminogen activator receptor and plasminogen activator inhibitor-1, a member of the urokinase plasminogen activator system, also play an important role in the tumor invasion process and are associated with either aggressive tumor characteristics or a poor prognosis in various

Table 4. Functional group analysis revealed the biological process in classifier genes

GO terms	3,269 genes	AO classifier (87 genes)	*P*	GB classifier (81 genes)	*P*
Biological process enriched in AO					
Neuron fate commitment	6*	3*	0.001	0*	—
Establishment of cell polarity	2	2	0.001	0	—
Nervous system development	84	8	0.002	2	0.619
Ion transport	57	6	0.004	3	0.168
Vesicle docking during exocytosis	6	2	0.011	0	—
Neurotransmitter transport	6	2	0.011	0	—
Potassium ion transport	22	3	0.021	0	—
Sodium ion transport	9	2	0.024	0	—
Synaptic transmission	42	4	0.026	1	0.649
Behavioral response to cocaine	1	1	0.026	0	—
Synaptic vesicle maturation	1	1	0.026	0	—
Exocrine pancreas development	1	1	0.026	0	—
Oligodendrocyte differentiation	1	1	0.026	0	—
Carotenoid biosynthetic process	1	1	0.026	0	—
Synaptic vesicle membrane organization and biogenesis	1	1	0.026	0	—
Negative regulation of microtubule depolymerization	1	1	0.026	0	—
γ-Aminobutyric acid catabolic process	1	1	0.026	0	—
Mast cell degranulation	1	1	0.026	0	—
Negative regulation of thymidylate synthase biosynthetic process	1	1	0.026	0	—
Dopamine metabolic process	1	1	0.026	0	—
Biological process enriched in GB					
Cell motility	48	0	—	8	0.000
Cell adhesion	105	5	0.148	11	0.000
Neuromuscular junction development	2	0	—	2	0.001
Antigen processing and presentation of exogenous peptide antigen via MHC class II	2	0	—	2	0.001
Peptide cross-linking	2	0	—	2	0.001
Cell surface receptor linked signal transduction	25	0	—	4	0.004
Immune response	61	0	—	6	0.004
Blood coagulation	17	0	—	3	0.009
Chloride transport	7	0	—	1	0.013
Inflammatory response	38	0	—	4	0.015
Humoral immune response	8	0	—	2	0.017
Erythrocyte maturation	1	0	—	1	0.024
Cholesterol homeostasis	1	0	—	1	0.024
T-cell selection	1	0	—	1	0.024
Positive thymic T-cell selection	1	0	—	1	0.024
Uridine metabolic process	1	0	—	1	0.24
Negative regulation of nucleotide metabolic process	1	0	—	1	0.024
Negative regulation of T-cell differentiation	1	0	—	1	0.024
Negative thymic T-cell selection	1	0	—	1	0.024
Regulation of smooth muscle contraction	1	0	—	1	0.024
Age-dependent response to reactive oxygen species	1	0	—	1	0.24
Creatine biosynthetic process	1	0	—	1	0.024
Regulation of proteolysis	1	0	—	1	0.24
Lymphocyte differentiation	1	0	—	1	0.024
Negative regulation of hydrolase activity	1	0	—	1	0.024
Peptide antigen stabilization	1	0	—	1	0.024
Immunoglobulin-mediated immune response	1	0	—	1	0.024
Fibrinolysis	1	0	—	1	0.024
Positive regulation of transcription factor import into nucleus	1	0	—	1	0.024
Arachidonic acid secretion	1	0	—	1	0.024
Negative regulation of membrane protein ectodomain proteolysis	1	0	—	1	0.024
Regulation of isoprenoid metabolic process	1	0	—	1	0.024
Leukotriene biosynthetic process	1	0	—	1	0.024
Response to superoxide	1	0	—	1	0.024
Release of cytoplasmic sequestered nuclear factor-κB	1	0	—	1	0.024
Granulocyte differentiation	1	0	—	1	0.024
Nucleotide catabolic process	1	0	—	1	0.024
Antigen processing and presentation of endogenous antigen	1	0	—	1	0.024

Abbreviations: GO, Gene Ontology database; AO classifier, classifier genes showing higher expression in anaplastic oligodendroglioma samples; GB classifier, classifier genes showing higher expression in glioblastoma samples.
*Number of genes belonging to the Gene Ontology terms.

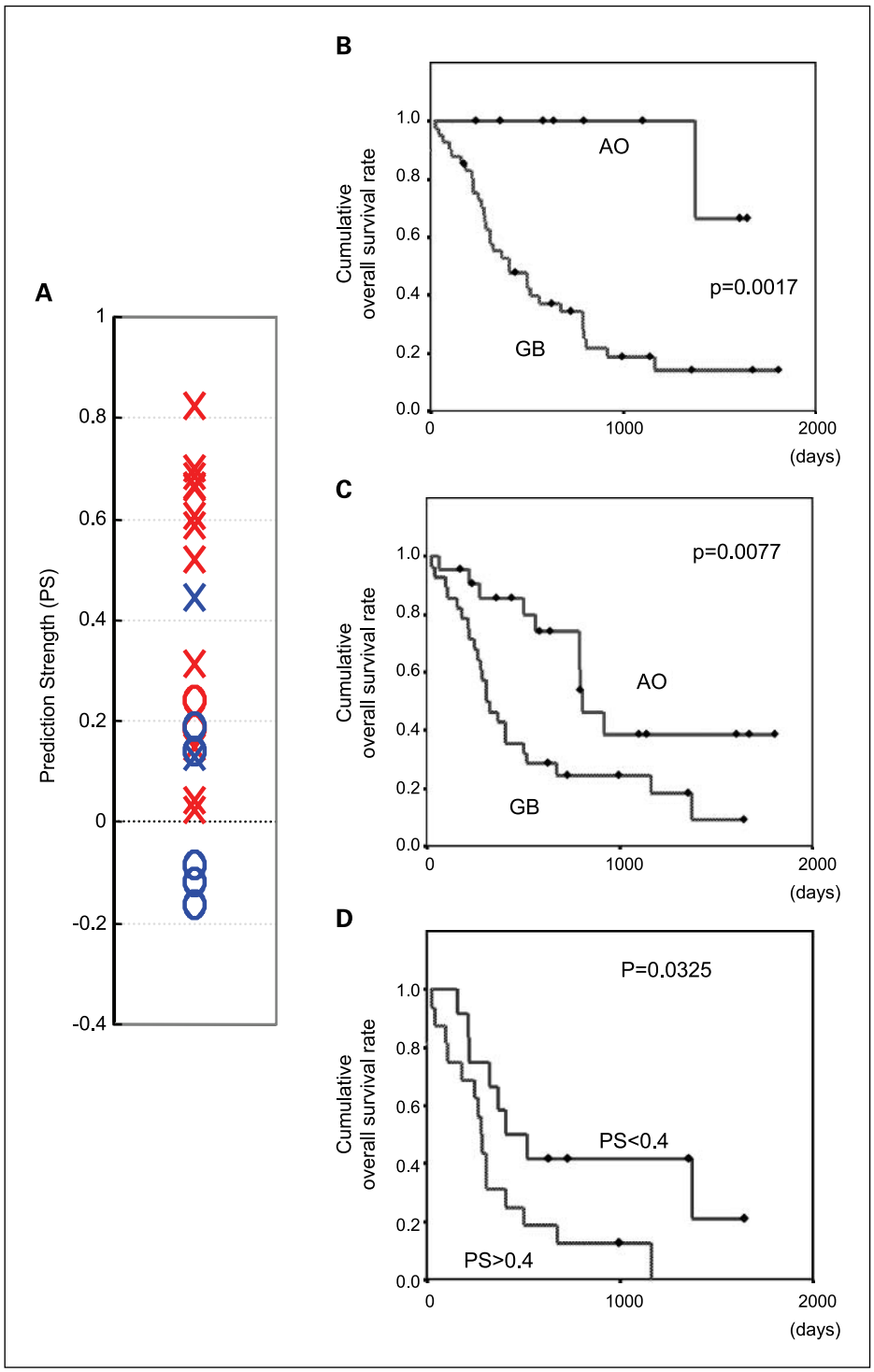

Fig. 2. Our molecular diagnosis system was applied to a MGH data set. *A,* the scatter plots show the PS values for the 21 classic malignant gliomas for which multiple neuropathologists were unanimous regarding the diagnosis. Red and blue, glioblastoma and anaplastic oligodendroglioma, respectively. ×, cases where overall patient survival was less than 2 y. *B* and *C,* Kaplan-Meier estimates of overall survival among all 50 malignant gliomas of a MGH data set. Classification according to (*B*) our molecular diagnosis system (*C*) histological diagnosis. *D,* Kaplan-Meier estimates of overall survival among 26 cases of histologically diagnosed glioblastoma in a MGH data set, stratified according to the PS with a cutoff value 0.4. *P* value was calculated with the use of the log-rank test.

malignancies, including gliomas (33–35). In addition to these genes, *Galectin-1* was also reported to be involved in the invasion process, and its expression displays a positive correlation with shorter survival among astrocytic tumors (36). Insulin-like growth factor binding protein 2 (*IGFBP2*) was frequently overexpressed in glioblastoma. IGFBP2 stimulates glioma cell invasion (37, 38).

Recently, several studies have shown the prognostic value of YKL-40 expression for poor outcome (21, 39, 40). It has been suggested to stimulate Ras and Akt pathways (41). Recent evidence indicates that the variation of glioma phenotype results from different kinds of alteration in signaling pathways. Phillips et al. (21) mentioned that YKL-40 expression and Akt activation were markers for poor prognosis among high-grade gliomas. As glioblastoma showed strikingly more YKL-40 expression than anaplastic oligodendroglioma by immunohistochemistry (42), YKL-40 stimulating signaling pathways may cause a highly invasive phenotype.

We note that our diagnostic model could not only discriminate between anaplastic oligodendroglioma and glioblastoma, but also disclose their distinctive molecular features. The characteristic function associated with clinical malignancy of glioblastoma is the invasion process, whereas classic anaplastic oligodendrogliomas had some extent of neuronal property. Using such representative functional features, it may be possible to refine the molecular diagnostic scheme.

It is interesting that a lower PS correlated with longer survival among the histologically diagnosed glioblastoma cases. From a pathologic point of view, Donahue et al. (43) reported that glioblastomas with some oligodendroglial characteristics showed a tendency toward better prognoses than pure glioblastomas. Our results showed the same phenomenon from a molecular point of view. Thus, glioblastomas whose gene expression signatures contained anaplastic oligodendroglioma components would show improved survival. These findings suggest the existence of molecular subclasses within glioblastomas.

Regarding the known molecular prognostic factors, we noted that the loss of 1p and 19q coexisted with MGMT promoter methylation in our anaplastic oligodendroglioma cases, as reported previously (44).

From a technical point of view, it is noteworthy that the results of our PCR array–based molecular diagnosis and those of microarray-based diagnosis were highly consistent with each other, especially for gliomas of histologically indeterminate diagnosis. Recently, the reproducibility of such large-scale gene expression analyses has come into question, particularly as pertains to the use of new methods such as the PCR array–based method we have adopted (45). Common concerns regarding these approaches arise from the statistical problems of handling such vast data sets as well as from the amount of unavoidable noise stemming from both intersample variation and from the techniques themselves. This study showed a clinically useful and reproducible ATAC-PCR–based molecular diagnostic system for malignant gliomas, which was shown to be comparable in effectiveness to systems based on microarrays.

Acknowledgments

We thank Chiyuri Maruyama, Satoko Maki, Keiko Miyaoka, and Mihoko Yoshino for their valuable technical assistance. A considerable part of this work was done in the Taisho Laboratory of Functional Genomics, Nara Institute of Science and Technology.

References

1. WHO Classification of Tumours of the Nervous System. In: Kleihues P and Cavenee WK (Eds) Pathology and Genetics Tumours of the Nervous System. Lyon: International Agency for Research on Cancer (IARC) Press, 2000.
2. Coons SW, Johnson PC, Scheithauer BW, et al. Improving diagnostic accuracy and interobserver concordance in the classification and grading of primary gliomas. Cancer 1997;79:1381–93.
3. Louis DN, Holland EC, Cairncross JG. Glioma classification: a molecular reappraisal. Am J Pathol 2001;159:779–86.
4. Cairncross JG, Ueki K, Zlatescu MC, et al. Specific genetic predictors of chemotherapeutic response and survival in patients with anaplastic oligodendrogliomas. J Natl Cancer Inst 1998;90:1473–9.
5. Muro S, Takemasa I, Oba S, et al. Identification of expressed genes linked to malignancy of human colorectal carcinoma by parametric clustering of quantitative expression data. Genome Biol 2003;4:R21. Epub 2003 Feb 27.
6. Kurokawa Y, Matoba R, Nagano H, et al. Molecular prediction of response to 5-fluorouracil and interferon-α combination chemotherapy in advanced hepatocellular carcinoma. Clin Cancer Res 2004;10:6029–38.
7. Iwao-Koizumi K, Matoba R, Ueno N, et al. Prediction of docetaxel response in human breast cancer by gene expression profiling. J Clin Oncol 2005;23:422–31.
8. Kato K, Yamashita R, Matoba R, et al. Cancer gene expression database (CGED): a database for gene expression profiling with accompanying clinical information of human cancer tissues. Nucleic Acids Res 2005;33:D533–6.
9. Matoba R, Kato K, Saito S, et al. Gene expression in mouse cerebellum during its development. Gene 2000;241:125–31.
10. Hegi ME, Diserens AC, Gorlia T, et al. MGMT gene silencing and benefit from temozolomide in glioblastoma. N Engl J Med 2005;352:997–1003.
11. Herman JG, Graff JR, Myohanen S, Nelkin BD, Baylin SB. Methylation-specific PCR: a novel PCR assay for methylation status of CpG islands. Proc Natl Acad Sci U S A 1996;93:9821–6.
12. Smith JS, Alderete B, Minn Y, et al. Localization of common deletion regions on 1p and 19q in human gliomas and their association with histological subtype. Oncogene 1999;18:4144–52.
13. Mariani L, Deiana G, Vassella E, et al. Loss of heterozygosity 1p36 and 19q13 is a prognostic factor for overall survival in patients with diffuse WHO grade 2 gliomas treated without chemotherapy. J Clin Oncol 2006;24:4758–63. Epub 2006 Sep 11.
14. Paunu N, Syrjakoski K, Sankila R, et al. Analysis of p53 tumor suppressor gene in families with multiple glioma patients. J Neurooncol 2001;55:159–65.
15. Mellinghoff IK, Wang MY, Vivanco I, et al. Molecular determinants of the response of glioblastomas to EGFR kinase inhibitors. N Engl J Med 2005;353:2012–24.
16. Storey JD, Tibshirani R. Statistical significance for genomewide studies. Proc Natl Acad Sci U S A 2003;100:9440–5. Epub 2003 Jul 25.
17. Golub TR, Slonim DK, Tamayo P, et al. Molecular classification of cancer: class discovery and class prediction by gene expression monitoring. Science 1999;286:531–7.
18. Wang Y, Klijn JG, Zhang Y, et al. Gene-expression profiles to predict distant metastasis of lymph-node-negative primary breast cancer. Lancet 2005;365:671–9.
19. Aoki T, Takahashi JA, Ueba T, et al. Phase II study of nimustine, carboplatin, vincristine, and interferon-β with radiotherapy for glioblastoma multiforme: experience of the Kyoto Neuro-Oncology Group. J Neurosurg 2006;105:385–91.
20. Nutt CL, Mani DR, Betensky RA, et al. Gene expression-based classification of malignant gliomas correlates better with survival than histological classification. Cancer Res 2003;63:1602–7.
21. Phillips HS, Kharbanda S, Chen R, et al. Molecular subclasses of high-grade glioma predict prognosis, delineate a pattern of disease progression, and resemble stages in neurogenesis. Cancer Cell 2006;9:157–73.
22. Mukasa A, Ueki K, Ge X, et al. Selective expression of a subset of neuronal genes in oligodendroglioma with chromosome 1p loss. Brain Pathol 2004;14:34–42.
23. Mukasa A, Ueki K, Matsumoto S, et al. Distinction in gene expression profiles of oligodendrogliomas with and without allelic loss of 1p. Oncogene 2002;21:3961–8.
24. Lu QR, Park JK, Noll E, et al. Oligodendrocyte lineage genes (OLIG) as molecular markers for human glial brain tumors. Proc Natl Acad Sci U S A 2001;98:10851–6. Epub 2001 Aug 28.
25. Ohnishi A, Sawa H, Tsuda M, et al. Expression of the oligodendroglial lineage-associated markers Olig1 and Olig2 in different types of human gliomas. J Neuropathol Exp Neurol 2003;62:1052–9.
26. Ligon KL, Alberta JA, Kho AT, et al. The oligodendroglial lineage marker OLIG2 is universally expressed in diffuse gliomas. J Neuropathol Exp Neurol 2004;63:499–509.
27. Wegner M. Expression of transcription factors during oligodendroglial development [review]. Microsc Res Tech 2001;52:746–52.
28. Stolt CC, Schmitt S, Lommes P, Sock E, Wegner M. Impact of transcription factor Sox8 on oligodendrocyte specification in the mouse embryonic spinal cord. Dev Biol 2005;281:309–17.
29. Mariani L, Beaudry C, McDonough WS, et al. Glioma cell motility is associated with reduced transcription of proapoptotic and proliferation genes: a cDNA microarray analysis. J Neurooncol 2001;53:161–76.
30. Leins A, Riva P, Lindstedt R, et al. Expression of tenascin-C in various human brain tumors and its relevance for survival in patients with astrocytoma. Cancer 2003;98:2430–9.
31. Goldbrunner RH, Bernstein JJ, Tonn JC. ECM-mediated glioma cell invasion [review]. Microsc Res Tech 1998;43:250–7.
32. Tran NL, McDonough WS, Donohue PJ, et al. The human Fn14 receptor gene is up-regulated in migrating glioma cells *in vitro* and overexpressed in advanced glial tumors. Am J Pathol 2003;162:1313–21.
33. Duffy MJ, Maguire TM, McDermott EW, O'Higgins N. Urokinase plasminogen activator: a prognostic marker in multiple types of cancer [review]. J Surg Oncol 1999;71:130–5.
34. Gondi CS, Lakka SS, Yanamandra N, et al. Expression of antisense uPAR and antisense uPA from a bicistronic adenoviral construct inhibits glioma cell invasion, tumor growth, and angiogenesis. Oncogene 2003;22:5967–75.
35. Muracciole X, Romain S, Dufour H, et al. PAI-1 and EGFR expression in adult glioma tumors: toward a molecular prognostic classification. Int J Radiat Oncol Biol Phys 2002;52:592–8.

36. Rorive S, Belot N, Decaestecker C, et al. Galectin-1 is highly expressed in human gliomas with relevance for modulation of invasion of tumor astrocytes into the brain parenchyma. Glia 2001;33:241–55. Erratum in: Glia 2001;35:166.

37. Wang H, Wang H, Shen W, et al. Insulin-like growth factor binding protein 2 enhances glioblastoma invasion by activating invasion-enhancing genes. Cancer Res 2003;63:4315–21.

38. Song SW, Fuller GN, Khan A, et al. IIp45, an insulin-like growth factor binding protein 2 (IGFBP-2) binding protein, antagonizes IGFBP-2 stimulation of glioma cell invasion. Proc Natl Acad Sci U S A 2003;100:13970–5.

39. Pelloski CE, Mahajan A, Maor M, et al. YKL-40 expression is associated with poorer response to radiation and shorter overall survival in glioblastoma. Clin Cancer Res 2005;11:3326–34.

40. Pelloski CE, Ballman KV, Furth AF, et al. Epidermal growth factor receptor variant III status defines clinically distinct subtypes of glioblastoma. J Clin Oncol 2007;25:2288–94.

41. Pelloski CE, Lin E, Zhang L, et al. Prognostic associations of activated mitogen-activated protein kinase and Akt pathways in glioblastoma. Clin Cancer Res 2006;12:3935–41.

42. Nutt CL, Betensky RA, Brower MA, et al. YKL-40 is a differential diagnostic marker for histologic subtypes of high-grade gliomas. Clin Cancer Res 2005;11:2258–64.

43. Donahue B, Scott CB, Nelson JS, et al. Influence of an oligodendroglial component on the survival of patients with anaplastic astrocytomas: a report of Radiation Therapy Oncology Group 83-02. Int J Radiat Oncol Biol Phys 1997;38:911–4.

44. Brandes AA, Tosoni A, Cavallo G, et al. Correlations between O^6-methylguanine DNA methyltransferase promoter methylation status, 1p and 19q deletions, and response to temozolomide in anaplastic and recurrent oligodendroglioma: a prospective GICNO study. J Clin Oncol 2006;24:4746–53. Epub 2006 Sep 5.

45. Hollingshead D, Lewis DA, Mirnics K. Platform influence on DNA microarray data in postmortem brain research. Neurobiol Dis 2005;18:649–55.